Thermochimica Acta, 193 (1991) 391–415
Elsevier Science Publishers B.V., Amsterdam

Conformational changes in nucleic acids/ chromatin structure

H.H. Klump [a,1], J. Völker [a], D.L. Maeder [a], Th. Niermann [b] and C.H.M. Sobolewski [a]

[a] *Department of Biochemistry, University of Cape Town, Rondebosch, Private Bag (South Africa)*
[b] *Biozentrum der Universität Basel (Switzerland)*

(Received 8 January 1991)

INTRODUCTION

The twelve topics listed below serve to structure the subject. They cover the work of many laboratories and it is unavoidable that the present review will omit some important papers. Due to the limited space allocated to this very broad subject we will only be able to highlight some more recent results. Detailed technical aspects will be neglected and the reader is referred to some recent reviews [1–3] and the literature cited therein.

Common to all topics in this paper is the focus, namely the quantification of interaction energies between biological entities, e.g. when the two strands of a DNA double helix come together or when nucleic acids and proteins come together in higher order structures of chromatin.

The development of a better understanding of biological processes at the molecular level and the evaluation of the energies involved will improve our ability to manipulate native conformations [4] or engineer new sequences which have desirable features, uncommon to the present biopolymers in the cell.

The investigations of conformational changes of nucleic acids and their constituents have flourished due to two new developments, first the improvement of the biochemical preparation techniques of native DNAs and DNA fragments which can be cut to size by restriction enzymes and can be isolated in great quantities, and second the improvement of the experimental techniques to determine the energetics of conformational transitions using highly sensitive scanning calorimeters [5].

The focus of interest has turned away from small cellular RNAs such as tRNAs back to DNA and DNA-like polynucleotides. In addition to the canonical conformers of double-stranded nucleic acids a few new structure

[1] Author to whom correspondence should be addressed.

0040-6031/91/$03.50 © 1991 – Elsevier Science Publishers B.V. All rights reserved

families have been established and attracted much attention, namely the closed circular conformations as they occur in plasmids [6], cosmids [7], and the natural DNA vectors [8] used in genetic engineering, the left-handed DNA [9] or Z-DNA conformation, the parallel DNAs [10], and the RNA-like DNA-pseudoknots [11]. In the following we shall discuss these new DNA structures in more detail.

The same new experimental approach has also been applied to the investigation of the elements of chromatin structure (to mono- and oligonucleosomes [12]) and [13] to chromatin structure in situ in isolated chromosomes and in the intact cell nuclei. We shall discuss the results of these thermodynamic investigations of higher order chromatin structure at the end of this review [14].

ENERGETICS OF HELIX COIL TRANSITION IN B-DNA

It is well established that under a given set of environmental conditions such as pH [15], the activity of monovalent or divalent cations [16] or added cosolvents [17] the relative stability of the B-DNA duplex structure depends on its primary structure, i.e. its base sequence; more precisely, the detailed conformation and hence the local stability depends primarily on the character of the next nearest neighbour base pair. Ten different nearest neighbour interactions have to be considered as important in any Watson–Crick type B-DNA structure [18]. These pairwise interactions are AA/TT, AT/TA, TA/AT, CA/GT, GT/CA, CT/GA, GA/CT, CG/GC, GC/CG, and GG/CC. The overall stability and the melting behaviour of any given B-DNA duplex structure can be predicted from its known sequence if this set of relative stabilities (ΔG) [1] and the temperature dependence (ΔH, ΔC_p) of the next nearest neighbour interactions is known.

Figure 1 gives the ΔG for the base pair formation in a B-DNA conformation as a function of the two most important environmental parameters, the sequence composition, and the sodium concentration.

The free enthalpy change can be calculated from the experimental values (transition temperature T_m, ΔH) for any given temperature T only by assuming the transition enthalpy is virtually temperature independent which can be justified from the observation of the absence of a sizeable increase of the heat capacity during the conformational change of the polymers. Thus

$$\Delta G_T = \Delta H_{cal}(1 - T/T_m)$$

The surface, which represents the free enthalpy change associated with the helix coil transition, calculated for 25 °C and per base pair, rises from the corner of low cation concentration and low GC content of the sequences considered to the range of physiological salt concentration and

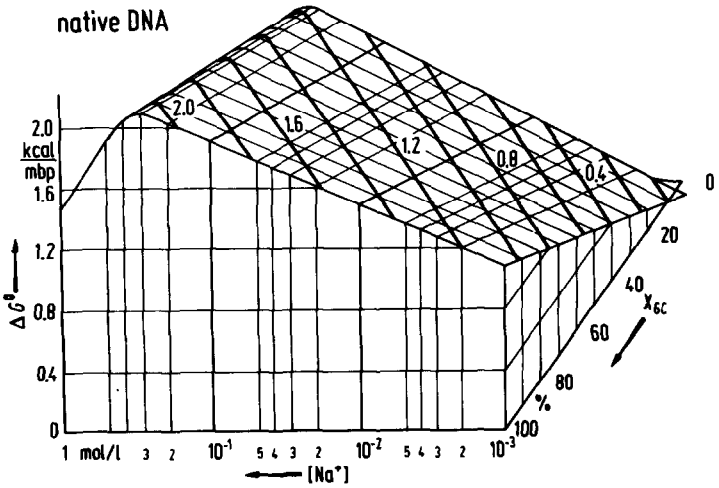

Fig. 1. The calculated standard Gibbs energy ΔG for the helix–coil transition of native DNA sequences as a function of the sodium concentration and the bulk sequence composition.

high GC content. Both variables (sodium concentration as well as GC content) contribute to the increase of ΔG. As can be seen from the diagram, the pure AT-sequence at 1 mM NaCl is not stable at room temperature. This proposal, derived from the property diagram, can immediately be tested experimentally to be correct. In fact Gruenwedel had reported this finding [19] based on his careful investigation on the counterion dependence of the transition enthalpy of poly d(A-T). The property surface is remarkably more tilted than the other three surfaces representing T_m, ΔH, and ΔS as a function of the sequence composition and the counterion concentration. For the first time the full set of thermodynamic state functions is available. The complete representation of the ΔG function allows us to evaluate the difference in stability between $(GGC)_n$ and $(GAT)_n$, e.g. for a given set of environmental conditions. For 10 mM NaCl and 298 K this difference amounts to 5.34 kJ mbp^{-1} (mol base pair), indeed very close to the value of 5.23 kJ mbp^{-1} reported by Kallenbach [20] for the corresponding RNA sequence.

The predictive tool of a set of thermodynamic state functions based on direct thermodynamic measurements can now be employed to predict the thermal stability of any synthetic or native polynucleotide sequence which exists in a B-DNA conformation. It can serve to discriminate between solvent effects and sequence effects on the thermal behaviour, and it can settle the discussion on the influence of the next nearest neighbours on the stability of a base pair, but the analysis of the contributions towards the B-DNA stability can be even more detailed and the individual forces that contribute to the stability of every single base pair can be separated [21].

DECONVOLUTION OF INDIVIDUAL FORCES THAT CONTRIBUTE TO THE STABILITY OF THE B-DNA CONFORMATION

The predominant interactions which contribute to the stability of the B-DNA structure are the following:

(i) Electrostatic interactions along the helix axis between consecutive heterocyclic bases either of the same strand or of the opposite strands (stacking interactions).

(ii) Hydrogen bonding within the planes of the individual base pair.

(iii) Hydrophobic interactions, supposedly originating from the energy required for the cavity formation in the water structure to accommodate the large polymer helix.

(iv) Coulomb interactions between the phosphate groups within the single strands and the phosphate groups of the opposite strands.

We shall try to discriminate between the impact of sequence- and solvent-effects on the stability of the DNA structure. The first point to discuss is the linear dependence of the transition temperature T_m on the net base composition of a DNA sequence, first discovered by Marmur and Doty [40], and in the following used to determine the base composition of any newly isolated DNA simply based on the melting temperature under standard conditions (standard saline citrate (SSC) buffer, ca. 150 mM Na^+).

A close inspection of the T_m versus log[Na^+] plots for different DNA sequences reveals a systematic decrease of the slope with increasing GC content. A linear extrapolation of the experimentally obtained T_m data results in an apparent common transition temperature T_m of 122 °C. The T_m differences, easy to detect and impressively large in some cases, however, should not be overestimated, for T_m is the most sensitive indicator of even minute conformational differences in the secondary structure. T_m differences as small as 2 °C are easily detectable. The corresponding free enthalpy difference ΔG is of the order of 0.17 kJ mbp^{-1}.

It is now readily accepted that the stability of a GC base pair surpasses the stability of an AT base pair by 7.1 kJ mbp^{-1}, and this value is well supported by various authors. Ornstein and Fresco [41] calculate 7.32 kJ mbp^{-1} by use of an empirical potential method. The extrapolated value (see Fig. 2) from the complete data set given here, results in 7.32 kJ mbp^{-1} for 1 mM Na^+ and 6.28 kJ mbp^{-1} for 100 mM Na^+.

Stacking interaction. Let us as a first approximation assume that the stacking enthalpy for AT base pairs is the same as for GC base pairs. The observed increase of the transition enthalpy per base pair is strictly correlated with the increase of the net GC content of a sequence. Since GC base pairs differ from AT base pairs only by one extra H-bond the difference in transition enthalpy (7.1 kJ mbp^{-1}) can be attributed to the contribution of this extra H-bond. Privalov et al. [5], investigating a different set of

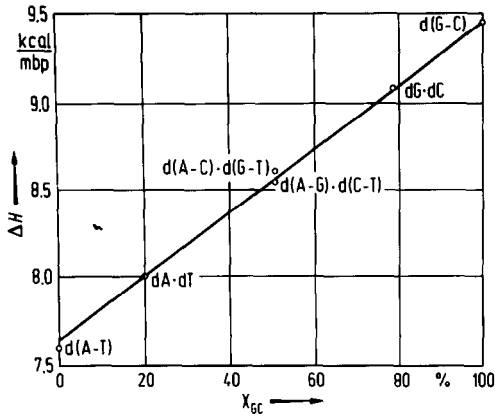

Fig. 2. Transition enthalpy per mole base pairs (mbp) vs. gross sequence composition. The enthalpy difference amounts to $\Delta H = \Delta H_{GC} - \Delta H_{AT} = 1.79$ kcal. The corresponding entropy difference $\Delta S = 1.3$ cal K^{-1}. The slope corresponds to the following equation $\Delta H_{GC} = 7.63(1 + 0.235 X_{GC})$ kcal mbp^{-1}.

biopolymers in aqueous solution, obtained a value of 6.3 kJ mbp^{-1} for a single H-bond. It is straightforward to subtract twice the enthalpy for a single H-bond from the transition enthalpy of an AT base pair and thrice this amount from the transition enthalpy of a GC base pair. The subtractions yield 17.6 kJ mbp^{-1} for ATs and 18 kJ mbp^{-1} for GCs. We can attribute the amount to the stacking enthalpy of an AT base pair or the GC base pair respectively. The simple approach outlined here leads to the conclusion that the two forces (stacking and H-bonding) contribute almost equally to the stability of the B-DNA conformation.

A closer look reveals, however, that the interaction of the two complementary strands cannot exclusively be based on the potential H-bonds. The predominance of the H-bonds for the discrimination between the canonical base pairs remains undisputed. Improper pairing consequently results inter alia in a decrease in conformational stability of the B-DNA [22,79]. One can approach the task of deconvoluting the different energetic contributions to helix stability by using a different theoretical model. If it is not for the different number of H-bonds in GC and AT base pairs, what else may serve to explain the observed enthalpy difference? The stacking free enthalpy ΔE is related to the cooperativity σ of the helix coil transition by the equation

$$\Delta E = RT \ln \sigma$$

We only have to know the magnitude of the cooperative parameter σ. One way to evaluate σ is from the average helix length $\langle n \rangle$ at $T = T_m$ using the relation

$$\langle n \rangle = \sigma^{-1/2}$$

TABLE 1

Contributions to the B-DNA structure stability

	ΔG (kJ mbp^{-1})	ΔH (kJ mbp^{-1})	ΔS (J mbp^{-1})
Integral value of all contributions	−3.76	−32.2	−98.65
Stacking	18.39	−17.56	+2.80
H-bonds and hydrophobic interactions	+14.63	−14.63	−101.45

We have shown earlier that $\langle n \rangle$ is the ratio of the van't Hoff enthalpy and the calorimetrically determined enthalpy per base pair. The resulting stacking free enthalpy yields −18.4 kJ mbp^{-1}. Gruenwedel [19] calculated 20.9 kJ mbp^{-1} for the stacking enthalpy in poly d(A-T) using a different theoretical approach. A statistical mechanical formalism was introduced by Go [22b]. It relates the degree of transition θ to the transition enthalpy ΔH, to the marginal loop size parameters α and β, and to the cooperativity σ.

$$(d\theta/dT)_{T_m} = 0.177\Delta H/RT^2(\alpha + \beta/2\sigma)^{-1/2}$$

The numerical calculation for the stacking free enthalpy in a polynucleotide helix yields −20.9 kJ mpb^{-1}, a value very close to −18.4 kJ mbp^{-1} given above.

The total free enthalpy change ΔG, based on the calorimetric data calculated for 298 K, amounts to 3.76 kJ mbp^{-1}. This value is in good agreement with other published results, e.g. from Privalov et al. for T_2 phage DNA (−5 kJ) based on a similar experimental approach [23], or with the results of Longuet-Higgins and Zimm [24] (−4.2 kJ), derived from a statistical mechanical approach. The different contributions to the B-DNA structure stability are summarized in Table 1.

The integral value of the transition enthalpy is an experimental result. Since the helix to random coil transition is regarded as a reversible process for DNAs also (only kinetically slowed down) the thermodynamic formalisms and definitions are valid.

The transition free enthalpy is calculated from T_m and ΔH under the assumption that the temperature dependence of ΔH is negligible.

The calculated entropy change ΔS due to stacking amounts to +2.80 J mbp^{-1}, a reasonable positive value due to an increase in local order in the system. The change in ΔS can be accounted for by changes in rotational degree of freedom along the backbone. Ross et al. [25] have measured the thermodynamic parameters for the association of a single strand to an existing double helix. The experimentally obtained entropy change ΔS is 54.5 J mol^{-1} of monomers, exactly half the amount the theory predicts for

the helix coil transition of double strands. The polyG system allows four-stranded helical structures to be formed. The resulting transition entropy ΔS per subunit yields 52.3 kJ.

It is far from accidental that the transition entropies (ΔS) give the ratio 4:3:2:1 if one takes the ΔS values of the four-stranded helix, to the three-stranded, the two-stranded and the single-stranded structures. Since the entropy change originates from the change in conformational freedom of single bonds along the polymer single strands it directly corresponds to the strandedness of the particular helix structure.

ENERGETICS OF ORDER–ORDER TRANSITIONS

Besides the temperature induced canonical helix coil transition, which can be taken as a prototype of an order–disorder transition there is a second group of conformational changes in helical polynucleotides which we shall term order–order transitions.

Depending on the environmental conditions and the sequence of the polynucleotides involved there are four alternative reaction schemes to bring about order–order transitions: (i) the inversion of the helical handedness from a canonical right-handed to a noncanonical left-handed conformation; (ii) the disproportionation of a double helix into a single strand and a triple helix; (iii) the addition of a single strand to a double helix; and (iv) the single–double strand displacement reactions, i.e. the displacement of one of the two strands of the helix by a matching single-stranded polynucleotide or the mutual exchange of one strand each between two helical structures. The first three reactions are considered reversible while the last reaction is obviously irreversible. Both ribo- and deoxyribo-polynucleotides can undergo these reactions. In the following we will discuss at least one example for each of these reactions.

Three biological reactions of fundamental importance, namely the replication, the transcription of the DNA double helix and the crossing over of DNA sequences between two chromosomes are considered to require strand separation prior to the consecutive steps in these processes. However the final state of the DNA under native conditions is always an ordered conformation, mostly a double helix, and sometimes a triple helix.

To discuss the unique features of order–order transitions in context we will choose the four AU homopolymer helices and the strictly alternating AU sequence as a model system. The five AU polymers in solution form stable double helical structures. The degree of hyperchromicity and the sharp melting profile indicate that in all these complexes there is a maximum degree of orientation, presumably due to the strict pairing of each adenine residue with a uridine residue. They show, however, marked differences in thermal stability. The invariable occurrence of displacement reactions between randomly coiled polypyrimidines or partly stacked poly-

purines and the homopolymer helices to form a helix of even greater thermal stability, indicate that these differences reflect differences in the thermodynamic properties of the helices. These considerations assume that the final state of all polynucleotides under study is the randomly coiled conformation, which is reasonable for high temperatures. It is also assumed that the transition entropy is similar for all double helix coil transitions. As was shown recently [2], this can safely be assumed. The entropy change per base pair reflects primarily the gain in rotational freedom along the backbone single strands upon denaturation of the helix. Hence differences in T_m correspond to differences in the transition enthalpy ΔH, and, if we assume that ΔH is also temperature independent, to differences in the free enthalpy change. Two sequences with identical GC content, which exhibit a different transition enthalpy per base pair, must have a different three dimensional structure in the helical state. A similar situation was found for the IC homopolymers. It is also observed that the thermodynamic stability of the double-stranded RNAs is always higher than the stability of the corresponding DNAs. The spontaneous course of the helix–helix displacement reaction such as dArU + rAdU rearranging to give rArU + dAdU indicates that the free energy change of the mixture of the hybrids is greater than that of the mixture of pure DNA- or RNA-like homopolymer helices.

The same also holds for the IC homopolymers. The displacement of one strand of the hybrid helix by an additional single strand of either type of polynucleotide to yield a homopolymer helix is governed by the same principle [26]. We can conclude that the displacement of the mRNA from the coding strand of the DNA is based on this thermodynamic phenomenon. The addition of a matching single strand to the homopolymer helix at elevated cation concentrations is thermodynamically driven.

The loss in conformational entropy of the single strand upon binding to the double helix is compensated by the gain in stacking and H-bonding energy once the electrostatic repulsion is decreased by the shielding of the phosphate groups by the cations [28]. Whether the triple-strand formation is actually possible is also dependent on the tendency of the homopolymer to form self-complementary secondary structures. Poly I, for example, has a pronounced tendency to form four-stranded helices at moderate cation concentration. This will prevent it from binding as a third strand to poly I poly C. This tendency for self-complementary structure formation is extreme for poly G [29]. All investigations on structures which contain poly G are obscured by this behaviour.

The temperature driven disproportionation reactions are completely reversible and also follow strictly the laws of thermodynamics.

Whether a disproportionation occurs is governed by the same set of rules as the addition of a third strand to the double helix. In the case of the disproportionation the third strand only originates from the second helix.

As is shown for the other order–order transitions in general the disproportionation temperature decreases with increasing cation concentration. This also holds for the inversion of handedness of the helical complexes formed from strictly alternating sequence. First it was the inversion of the CD signal which suggested an inversion reaction [30]. Later the absolute configuration was proven for the oligomeric analogue by X-ray structure analysis [31]. For quite a while it was thought that inversion is only possible for deoxy polymers. Now we have a growing list of various copolymers which can form a left-handed helix under appropriate conditions, i.e. higher counterion concentration and/or reduction of water activity. The energy required for the inversion is surprisingly low (about 4 kJ mbp^{-1}) [27]. The only reason why the polymer is not oscillating between the two conformational states is that the inversion is a highly cooperative process; there is only one inversion-centre in each helix, and its formation requires a large activation energy.

PARALLEL DNA

Watson–Crick base pairing seems to be incompatible with parallel stranded helix formation; however, alternative conformations are feasible. There is experimental evidence for parallel stranded duplexes stabilized by, (i) hemiprotonation of C, (ii) protonation of poly A, and (iii) introduction of bulky substituents (X) in poly (x^2A) poly U. Triple helixes also have been shown to be associated in a parallel orientation of the second pyrimidine strand which is stabilized by Hoogsteen base pairing in the major groove. These triple helixes either originate from disproportionation reactions of homopolypurine/polypyrimidine helices when adenine is the purine, or from binding of homopyrimidine deoxyoligonucleotides to the major groove of homopyrimidine/homopurine tracks in DNAs. Pattabiraman [32] reported a force field calculation which indicates that a parallel right-handed structure with reversed Watson–Crick base pairing could be energetically as favourable as the conventional antiparallel B-form DNA. This local triple helix formation can be utilized, presuming that the oligomer bears a chemical cleavage function, to design custom made "restriction elements" to cut total genomes into predetermined large sequences of DNA [33]. The possibility of protecting a piece of DNA or RNA from enzymatic degradation by aligning a complementary nucleotide sequence in parallel to the purine sequence and making it inaccessible for any repair enzyme or for transcription is to be explored as an effective way to stop, for example, the proliferation of the HIV genome. In a recent paper Germann et al. [33] have given the first set of thermodynamic data which can be utilized to compare the energetics of parallel stranded DNA formation to the formation of canonical DNA structures. Table 2 gives the data set for the nucleation and the propagation step involved in forming a parallel and/or antiparallel helix [33].

TABLE 2

Thermodynamic data for the helix coil transition of alternating parallel and antiparallel AT hairpin structures [a]

Sequence	T_m (°C)	ΔH_{vH} (kJ mol^{-1})	ΔS^0 (J mol^{-1} K^{-1})
3′-d(AT)$_4$ C$_4$ (AT)$_4$ 3′	36.6	106	343
3′-d(AT)$_5$ C$_4$ (AT)$_5$ 3′	39.3	137	441
5′-d(AT)$_5$ C$_4$ (AT)$_5$ 3′	57.2	244	738
5′-d(AT)$_5$ T$_4$ (AT)$_5$ 3′	58.4	229	690

[a] Melting temperatures were recorded in 0.8 M NaCl, 0.1 mM EDTA, and 10 mM phosphate, pH 7.

FORMATION OF A DNA PSEUDOKNOT

There are five different ways to form triple stranded helices from oligonucleotides (Fig. 3 (A—E)). These are, (i) mixing a homopurine oligonucleotide with its complementary homopyrimidine oligonucleotide in the stoichiometric ratio of 1:2 (see Fig 3(A)) [34], (ii) addition of a complementary homopyrimidine guest strand to a host hairpin helix with a homopurine–homopyrimidine stem region (Fig. 3(B)) [35], (iii) addition of a complementary homopurine strand to a palindromic homopyrimidine sequence (Fig. 3(C)) [36] (this triple helix can serve as a model for the central section of the H-DNA structure [37]), and finally (iv) a triple helix is formed by successive folding of a single continuous oligonucleotide sequence (Fig. 3(D–E)) [38]. Triple helices formed from a single continuous oligonucleotide sequence satisfy the characteristics of a pseudoknot.

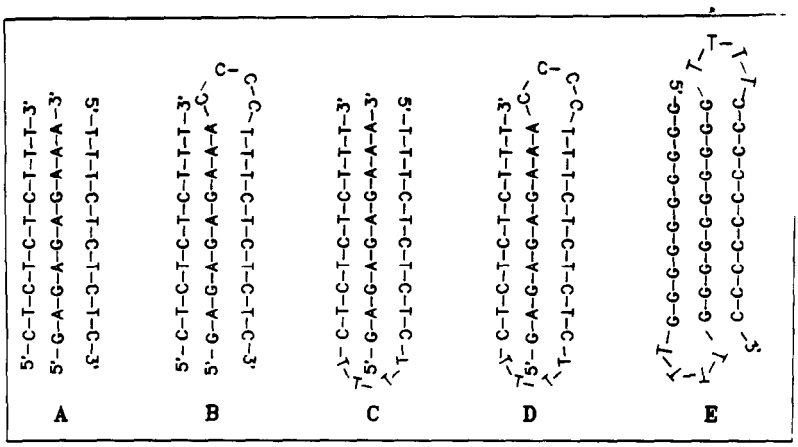

Fig. 3. Schematic triple helix formation from (A) three, (B, C) two, or (D, E) one oligonucleotide strands.

We used a 38mer oligonucleotide with the sequence

d(5′-GAGAGAGAAACCCCTTTCTCTCTCTTTTCTCTCTCTTT-3′)

which is henceforth referred to as JV-ITS. The characterization of the secondary structure of each state of JV-ITS was based on a variety of spectroscopic methods (CD, UV, and fluorimetry). Under appropriate conditions (temperature, pH) it was also possible to detect DNA oligomer hairpins and pseudoknots using a gel migration assay.

The results can be summed up as follows: using UV spectroscopy, CD spectroscopy, fluorescence enhancement by ethidium bromide binding, nondenaturing gel electrophoresis and differential scanning calorimetry we have shown that the oligonucleotide JV-ITS undergoes two consecutive, distinctly different, pH-dependent, folding steps from a random coil into a pseudoknot. The experimental results presented here are in agreement with the proposal that the first step at pH 8.0 leads to a hairpin structure with a 3′ dangling oligopyrimidine end while the second step at pH 5.5 completes the DNA pseudoknot formation. At pH 5.5 there is some evidence for the appearance of an alternative intermolecular bulge–loop structure in a concentration dependent equilibrium with the pseudoknot [39].

The thermodynamic properties of the pseudoknot in 100 mM [Na^+] were, $T_m = 69\,^\circ C$, $\Delta H_{vH} = 502$ kJ mol^{-1}, $\Delta H_{cal} = 619$ kJ mol^{-1} and those of the hairpin were, $T_m = 63\,^\circ C$, $\Delta H_{vH} = 310$ kJ mol^{-1}, $\Delta H_{cal} = 331$ kJ mol^{-1}. At high oligonucleotide concentrations the intramolecular triple-stranded structure was found to be in equilibrium with an intermolecular triple-stranded bulge–loop structure. Gel mobility shift analysis revealed that the pseudoknot migrated faster than the hairpin due to its compactness.

THERMODYNAMICS OF DNA SUPERCOILS: SIZE AND SEQUENCE DEPENDENCE

It is commonly accepted that negative supercoiling is accompanied by a local destabilization of a corresponding number of base pairs [42]. This suggestion is based on the finding that premelting of a fraction of base pairs seems to occur at distinctly lower temperature as compared to the gross/overall melting of the bulk ordered polynucleotide. Such premelting is not observed in our experiments and we assume that melting curves in the presence of high concentrations of denaturants which show this effect do not correspond to an unperturbed transition. If premelting does occur, the melting curves of the plasmid pZmc134 rather indicate premelting directly at the beginning of the observed steep linear increase of absorption of the supercoiled (sc) form. The small step on the transition curve could only be observed for sc pZmc134. In all other cases the concentration of

DNA was very low and the expected signal might be obscured by the instrumental noise. Wherever premelting may occur on the temperature scale, negative supercoiling can directly diminish the thermal stability of only a very small number of base pairs [43].

However, neither the mutual influence of separation of basepairs and writhing on an unwound DNA strand is known, nor is it known if a change in the linking number is evenly distributed between twist and writhe. Conformational transitions could be even more complex if inversion between right-handed and left-handed DNA is considered, which is quite common in plasmids. Obviously negative supercoiling increases the thermal stability of the base paired DNA double strand.

Which geometrical model of supercoiled DNA can serve to explain the proposal that negative supercoiling and increased thermal stability are positively correlated? In closed circular (cc) DNA topological stress arises when the linking number of the single strands deviates from that of the relaxed cc form [44]. This counteracts the tendency of DNA to adopt its naturally occurring twisting. These two conformational effects influence the axial writhing of DNA. Unwinding of DNA double strands by DNA gyrase action produces tertiary coils, which means that the DNA strands are increasingly supercoiled. An increasing stress in the DNA strands by further local unwinding winds the residual DNA strands evenmore strongly around this axis, which means that it gets more and more difficult for the DNA double strands as well as for the DNA single strands to leave this region. This entanglement is the main cause for a topological hindrance for the separation of base pairs via loop formation of the single strands. This has to be considered for the explanation of delayed melting of negatively supercoiled DNA. Thus one can imagine that the torsion of the strands around the superhelix axis will affect the equilibrium between the ordered and disordered state [45]. The melting of a nicked and a closed circular (cc) DNA is different due to the lack of free spinning ends in a cc form. It is known that increase of temperature interferes with a decrease of the twisting (unwinding) of the double strand. Because the linking number Lk is fixed in cc DNA this has consequences for the geometry of a negatively supercoiled DNA [46]. Unwinding upon heating could decrease the twisting of the DNA until the topological stress is relieved. From this reasoning it seems to be obvious that in negatively sc DNA the basepairs are not necessarily destabilized and that long range self stabilizing effects are based on this special geometry.

We can correlate $dT/d \log[Na^+]$ with the ring size of DNA and the topological stress to which it is submitted (see Fig. 4). If different thermal stability would exclusively reflect the topological stress in the sc DNA conformation, one could only expect a constant offset of the T_m values. However, as compared to the $dT_m/d \log[Na^+]$ [47] ratio of nc DNA there is also a different relative dependence on the salt concentration. We

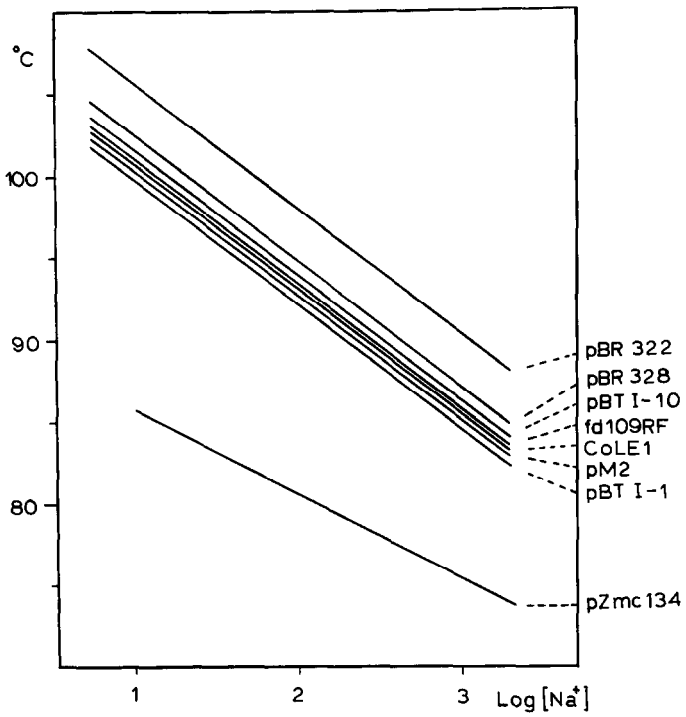

Fig. 4. Transition temperature T_m vs. log[Na^+] for supercoiled DNA from pBR322 (2.88 megadalton), pBR328 (3.23), pBT I-10 (5.10), fd109RF (5.50), CoLE1 (4.2), pM2 (6.3), pBT I-1 (7.3), and pZmc134 (13.8).

assume that the melting behaviour of DNA is also dependent on the pathway the double helix axis describes in space. Thus it should be possible to discriminate between the coiling of the double helical DNA along its full length (solenoidal) and a toroidal coil. The solenoidal DNA superhelix conformation is a unique structure which should influence the polyelectrolyte properties of DNA. Coiling of the double strands around themselves could result in close contacts of equally charged groups, thereby excluding the cations from the interface and an overlapping of the counterion spheres along the superhelix axis.

A systematic topological and geometrical impact on conformational stability and thermal denaturation of negatively supercoiled DNA is investigated by UV absorption spectroscopy and adiabatic scanning calorimetry. Eight supercoiled DNA species ranging in molecular weight from 2.9 to 13.8 megadaltons are compared. The evaluation of the integral melting curves reveal linear $dT_m/d \log[Na^+]$ plots for each of the species (see Fig. 4). The sc DNA molecules are suspended in NaCl solutions which are submitted to N_2 pressure of about 10 bars to shift the boiling point of the solvent H_2O to 160 °C. From the slope of the UV-melting curve at $T = T_m$ the van 't Hoff (apparent) enthalpy can be calculated. The true transition

enthalpy per base pair is determined by the help of a differential adiabatic scanning calorimeter. The ratio of the van 't Hoff enthalpy ΔH_{vH} and the calorimetrically determined enthalpy ΔH_{cal} reveals a DNA superhelix coil transition which has a comparable, if not even higher, cooperativity than the helix coil transition of linearized DNA [48]. It is clearly demonstrated that the thermal stability of supercoiled DNA is influenced by the ring size of the DNA species and the topological stress to which it is submitted. The linear charge density calculated for the supercoiled DNA is compatible with a model of a solenoidal rather than a toroidal unwound superhelical conformation.

THERMODYNAMIC BASIS OF THE GENETIC CODE

The genetic code is degenerate but alternative synonymous codons are generally not used with equal frequency. There is a close correlation between observed codon frequencies and codon/anticodon interaction free energies which will be outlined in this section [49].

The pattern of bias is broadly similar in genes from a single species or taxonomic group. In the two best studied organisms, namely *Escherichia coli* and *Saccharomyces cervisiae*, genes differ largely in the degree of bias rather than its direction [50–52]. These data may provide evidence suggesting the generality of certain phenomena, e.g. the high speed of transcription/replication in unicellular organisms or the single-strandedness of certain phage DNAs.

As will be discussed in some detail here, closely related organisms have similar patterns of codon usage. For example, with respect to codon usage, *Salmonella typhimurium* closely resembles *E. coli*, while all mammalian species so far examined (mouse, rat and cow) largely resemble humans. Included in our considerations are also plants, a fungus with an extremely low GC content, and single-strand phage DNAs.

There are various approaches discussed in the literature aiming to explain the obvious fact that codon usage is highly biased. The different concepts put forward can be termed (1) the "optimization of translation kinetics" concept, (2) the "need to have a uniform double helix stability" concept, (3) the "mRNA secondary structure" or "transcriptional efficiency" concept, and (4) the "most abundant tRNA codon choice" or "translational efficiency" concept [53–57].

We favour a variation of the second concept which we shall call the "codon/anticodon interaction free energy" concept which can be demonstrated to underline some of the other concepts as well. Looking at interaction free energy can serve to explain various strategies of unicellular and multicellular species. In the following we shall discuss three observed strategies in more detail.

The first strategy is observed for eucaryotes, and a clear-cut picture

emerges from viewing codon preferences listed for human genes. Humans tend to follow Oscar Wilde's definition of simple taste; they only go for the best. Choosing codons with highest interaction free energies is equivalent to choosing the most accurate pairing, especially with respect to the third (wobble) position. The most accurate pairing is equivalent to the longest residence time for the codon/anticodon reading; this inevitably leads to the slowest transcription rate [58]. Mammals/humans can cope with this. Bacterial gene sequences engineered to contain these preferred eucaryotic codons are transcribed more slowly than the same gene sequence composed from preferred bacterial codons. There are variations of this strategy but the take home message seems to be that eucaryotes go for precision. Their prime aim is to keep the large genome as intact as possible. The principle seems to be violated in the eucaryotic codon choice when there is a C followed by a G either within the same triplet, or, though less pronounced, between triplets. It was observed that most higher eucaryotes (but not insects) show a selective deficiency in the dinucleotide pair 5′C-G3′. The explanation for the deficiency put forward [59] is that these C residues are methylated and as a consequence hypermutation of the methyl-C leads to the elimination of C-G dinucleotides [60]. Inspecting human codon frequency tables shows, for example, that the two Arg codons AGA and AGG are preferred over the "best" Arg codons CGC and CGG, because of the C-G neighbourhood in the latter. The preferred Ser codon is AGC instead of UGC, and this avoidance of intracodon C-Gs is obvious also from the selection rules visible in the following three quartet codons such as the preference of the codon ACC instead of ACG for Thr, CCC over CCG for Pro, and GCC over GCG for Ala.

We can also include the intercodon C-G dinucleotides in the discussion. Inspecting the published codon preference tables of eucaryotes shows that the frequency of codons NNC is 0.35 and GNN is 0.31. The expected intercodon frequency of C-G is thus 0.11, whereas the observed frequency is 0.055. For example the codon utilization of histidine is 58% CAC and 42% CAU. This distribution reverses if the following codon starts with G. The frequency of CAC drops to 37% and the frequency of CAU rises to 63% [61].

There is no tendency visible for the selection of the third letter of a codon to counterbalance the general GC content of the first two letters of each codon to confer a balanced GC content. The percentage GC of the total human genome is about 42% GC, while the mean value calculated from the list of preferred codons amounts to 63%. This tendency is even visible for an extreme case [62], the genome of the fungus *Dictyostelium discoideum*, which has a T_m-derived GC content of only 25% but a codon preference based GC content of 35%.

The alternative strategy is obviously to choose codons with intermediate stability. Precision may be sacrificed but what is gained is speed. Choosing

codons with intermediate interaction energies leads immediately to a gene with intermediate and uniform stability around an individual characteristic mean stability value. The particular codon preference is biased by the gross GC content of the gene sequence chosen for the investigation. The third letter of each codon in a coding sequence of a bacteria plays the decisive role in producing the homogenous stability distribution along the entire gene sequence, in other words [63] the redundance at the wobble third base counter-balances the G + C content variation at the first and second bases of preferred codons. This can be readily demonstrated by calculating the mean GC content of the seventeen preferred codons (not counting the codons for Met and Trp). The mean value calculated from codon preferences for *E. coli* amounts to 48.2% GC compared to 50% for the total *E. coli* genome. The mean value for *Bacillus subtilis* amounts to 41.2% GC calculated from the codon preference list which is almost exactly equal to the 42% GC calculated from T_m for the total genomic DNA. The results for *Thiobacillus ferrooxidans*, which has a T_m-derived G + C content of 62% yields 59% GC content computed from the list of preferred codons for this bacterial genome. The preferred codons are basically always codons of intermediate stability and the frequency of G or C in the third position of each of the preferred codons serves in addition to counterbalance the average local GC frequency at the first and second sites in a gene. This strategy is adopted by procaryotes and serves the main purpose to trade accuracy in gene expression, which is so important for large genomes of eucaryotes, against high efficiency and speed whenever the nutrition supply becomes favourable. There is no avoidance of C-G neighbourhoods. Neither intercodon nor intracodon C-Gs are selected against. Whatever the reason might be for the higher eucaryotes to avoid this (possibly some regulatory role of the methylated/nonmethylated C next to the G) this selective pressure is absent in procaryotes [64].

In unicellular organisms, the highly expressed genes use a smaller subset of codons as compared to the genes, which are much more weakly expressed. A survey of 165 *E. coli* genes reveals a positive correlation between high expression and increased codon bias. A similar trend is described for the codon selection in yeast. Codon usage in the highly expressed genes correlates with the abundance of isoaccepting tRNAs in both *E. coli* and yeast. The good fit of the preferred codon usage to the isoacceptor tRNA abundance explains the observed high translation level and the high steady state level of these proteins. The resulting correlation hints at convergent evolution of the tRNA genes and the species-specific codon choice. This codon dialect as it was called by Ikemura [65], however, is not the consequence of the abundance of a given set of abundant tRNAs. Any correlation between the codon usage profile and the secondary structure of the transcribed mRNA is only a chance event. Currently we are unable to put forward any rule correlating mRNA secondary structure, let

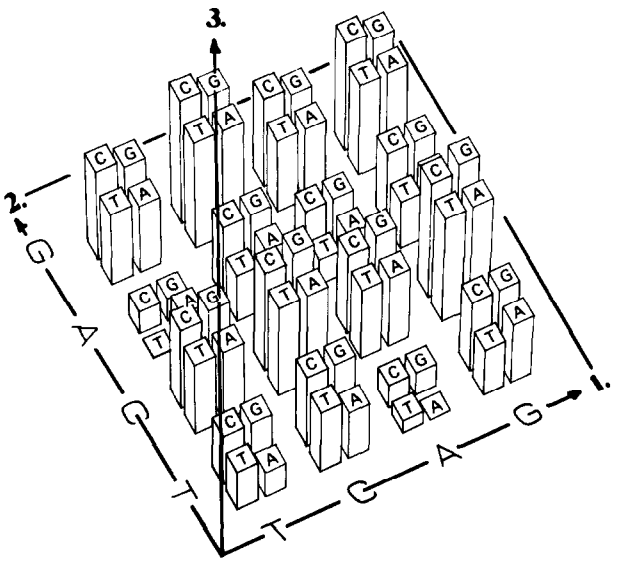

Fig. 5. Genetic code matrix. The heights of each column correspond to the codon/anticodon interaction free energy ΔG.

alone tertiary structure, and translation efficiency. The third type of a straightforward strategy can be derived from the list of preferred codons observed for the single-stranded viruses. They obviously select for the least stable codon/anticodon pairs, unrelated to the GC content of their hosts, to secure their single-strandedness in the first place.

Expanding the analysis to plants the observation is [66] that the nuclear genome follows the first strategy while the chloroplast DNA reflects the second strategy. More specifically one finds that monocotyledons share the most commonly used codon for only one of eighteen amino acids while dicotyledons share the most commonly used codons of chloroplasts in only four of eighteen amino acids. In general, the chloroplast codon profile resembles that of unicellular organisms, with a strong bias towards the use of A/T in the wobble position. Figure 5 gives a representation of the codon table as a column diagram, where the height of each column represents the codon/anticodon interaction free energy.

SATELLITE DNAS

The idea of introducing calorimetry as an analytical tool emerged from the observation that the experimental transition curve of calf thymus DNA, scanned in an adiabatic differential calorimeter, showed a complicated but remarkably reproducible pattern of individually distinguishable peaks. This pattern was obtained regardless of the source of the sample. It turned out

to be identical to the pattern of the same DNA, obtained by Blake and Lafoley [67] with the help of differential UV melting. It was also very similar to the UV absorbance profile from buoyant density gradient centrifugation, which sorts the sheared DNA fragments according to their GC content. The pronounced superstructure of the calorimetric transition curve is far from accidental. It reflects the relative population of the sequence composition of the cooperative units along the calf genome [68].

These sequences reveal a large variety of thermal stabilities, and the superposition of the individual sequences results in the envelope of the complete melting curve. The presence of highly repetitive short and homogeneous sequences such as the so called satellite DNAs, which turn out to be related to the individual peaks sticking out from a broad transition in calf thymus DNA, is clearly demonstrated in this scan. To originate such characteristic peaks the domain (satellite) has to fulfil two conditions: (i) the number of identical repeats of this particular domain has to be substantial, i.e. the concentration of this sequence has to be of the order of 2–3% of the total DNA, and (ii) the length of the domain must be of the order of the cooperative length of the bulk DNA, namely 50 to 100 base pairs. We take the temperature at the peak maximum as a measure of the base composition of the domain underlying the peak, following Marmur and Doty's finding of a linear dependence of the transition temperature of the gross GC content of a sequence [40]. Thus from the number and relative positions of the extra peaks the number and compositions of the satellite DNAs of a given animal species can be determined, even in a heterogeneous mixture of the unfractionated bulk DNA. The large number of different unique sequences, i.e. single copies of genes, is represented in the large unsymmetric denaturation peak which stretches over the full range of the transition interval. The enthalpy per base pair, the transition temperature, the axial phosphate distance along the helix axis, and the free enthalpy difference at a given set of environmental conditions can be utilized to identify a given DNA according to its G + C content. All four physical properties mentioned above are linearly dependent on the sequence composition and reflect only the next nearest neighbour interactions. A typical calorimetric transition curve of calf thymus DNA is given in Fig. 6.

TOPOLOGICAL GENE SWITCHES

Reversible modification of the conformation of genomic DNAs offers attractive possibilities of switching gene activity on or off as needed for cell function. As an example, the methylation and demethylation of cytosine residues in a DNA has been related to gene expression [69] in a number of genes. As one of the many possible parameters controlling the expression of the genetic information it has been suggested that certain genes in

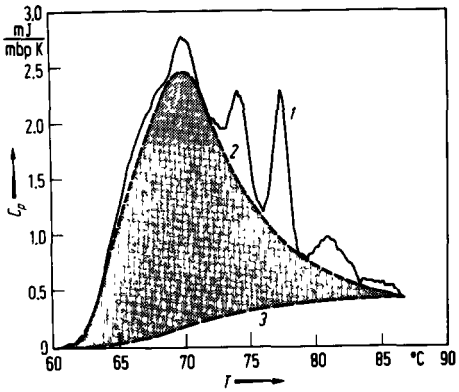

Fig. 6. Apparent heat capacity as function of the temperature for calf thymus DNA (1). The shaded area (2) represents the transition enthalpy of a total genomic DNA from a species which lacks satellite DNA sequences (chicken).

nonexpressing cells are highly methylated in their 5′-flanking regulatory regions (promoter regions) but become hypomethylated when the gene is activated. We have demonstrated in a series of preliminary experiments, that it is possible to invert the helical handedness for a series of model polynucleotides as well as for part of the native DNAs, as long as there is a sufficiently long stretch of alternating purine/pyrimidine base pairs present. Furthermore it can be shown that the extent of methylation of the cytosine rings in a given sequence is a key feature which strictly determines how significant changes of the environmental conditions are required to make the helix invert its handedness [70].

It is tempting to propose the following hypothesis. The gene regulation can be brought about by a switch in the spatial arrangement of the DNA sequence from the right-handed B-DNA conformation to the left-handed Z-DNA conformation. This switch can be set by the extent of methylation, by localized DNA supercoiling to drive the structural transition, by protein binding to the left-handed conformation or by a combination of these factors.

There is another group of hypothetical gene switches which involve tertiary structure elements such as triple strand formation as in H-DNA [71], loops, and pseudoknotting. A pseudoknot involves intramolecular pairing of bases in a hairpin loop with a few bases outside the stem of the loop to form an additional stem and loop region. Little is known about the spatial structures and the thermodynamics of interactions involved in the tertiary structure of the DNA. Bifurcations, cruciforms, and triple strands are also possible intermediates to be considered as regulatory elements either by their special property of keeping the two strands of the double helix apart for some time or by their protein binding capacity.

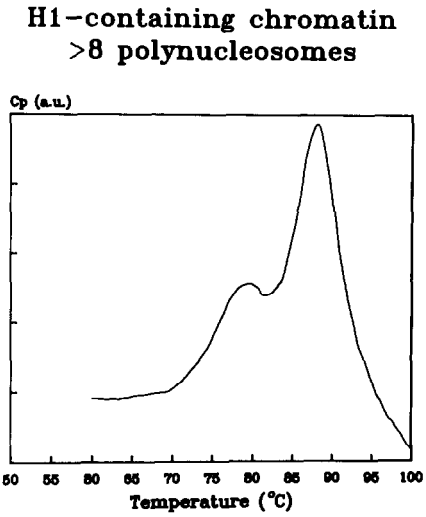

Fig. 7. First derivative of the A_{260} vs. temperature for polynucleosomes (8mers) in the presence of H1.

THERMAL STABILITY OF CHROMATIN SUBUNITS

The standard methods for spectroscopic chromatin analysis depend on the optical clarity of solutions, a condition unfit for investigating nucleosomal arrangements in chromosomes or nuclei, not to mention complete cells. Therefore all studies on nucleosomes and higher order chromatin structure have been carried out at low ionic strength on isolated core particles [72] or chromatin that has been rendered soluble by nuclease digestion. The soluble chromatin is in fact a mixture of polynucleosomes of various sizes. It is obvious that such studies will not reveal the true structure of native chromatin, while unfractionated and untreated cells would guarantee the chromatin structure to be native.

We will demonstrate in this section [73], that the nucleosomal structure is a conserved building block which remains essentially unchanged throughout the increasingly complex structures of DNA/histone complexes (see Fig. 7). Its conservation can be shown from the comparison of the melting profiles of these entities either recorded by UV absorbance or by heat capacity measurements as a function of the temperature, giving rise to the claim that the underlying structures are very similar to nucleosomes. The assignment of the different peaks of the thermal denaturation profiles is based on spectral analysis and on biochemical modifications [74]. Higher order chromatin structure, if present, is stabilized entropically rather than enthalpically. There is no peak visible in the denaturation pattern of oligonucleosomes, which can be assigned to an endothermic cooperative conformational change, which may be due to higher order structures.

Nucleosomes

The thermal denaturation of the nucleosomal core particles is included here for comparison only, to distinguish between the contributions of the fundamental building block of chromosomal structures, the core particle, to the thermal denaturation pattern of the more complex structures and the contributions from higher order structure elements. The results obtained in this study correspond very well with previous results of Weischet et al. [72]. Figure 7 gives the first derivative of the thermal denaturation curve of core particles recorded at 260 nm as function of the temperature. The scan shows clearly that the denaturation proceeds in two discrete steps, a minor step around 58 ° C and a major step around 71 ° C. The same two steps are observed in the corresponding calorimetric scan, which monitors the change in heat capacity ΔC_p versus temperature. It is readily accepted that the first minor step corresponds to the structural transition of a part of the DNA from the nucleosomal core while the bulk of the DNA melts simultaneously with the protein attached. The complexed denatured protein prevents the DNA renaturing. The independent melting of the two domains of the core particle, the 40 base pairs from the ends of the DNA wrap and about 100 residual base pairs of the DNA together with the core histones, will be a landmark in all consecutive denaturation curves. The CD melting will be used as an additional source of information to discriminate between the protein denaturation and the melting of the DNA. Table 3 gives a summary of all melting experiments, including the transition temperature, the hyperchromicity, and the thermodynamic parameters.

TABLE 3

Thermodynamic and spectroscopic parameters for the thermal denaturation of core particles, soluble chromatin and metaphase chromosomes

	T_m (° C)	h [a] (%)	ΔH (kcal mbp^{-1})	ΔS (cal mol^{-1} K^{-1})	$\Delta G^{\ominus}$ (kcal mbp^{-1})
Core particles					
Premelting	61	26	7.5	22.3	0.84
Melting	76	74	12.1	34.8	1.80
Soluble chromatin					
Premelting	70	27	7.6	22.1	0.85
Melting	84	73	12.0	33.7	1.86
Metaphase chromosomes					
Premelting	74	23	7.8	22.5	0.87
Melting	89	77	12.4	34.3	1.90

[a] Observed hyperchromicity is about 40%. The value in this table gives the relative fraction for the two steps.

Polynucleosomes

The melting curve for polynucleosomes is shown in Fig. 7. It is in all respects very similar to the melting of the isolated core particles. The calorimetric measurements were run in the following way. For the first scan both cells contained the same buffer to establish a secured and reproducible baseline. In the second run the buffer of the sample compartment was exchanged for the polynucleosome solution in the same buffer. The scan was started at 4 °C not to miss any cooperative transition which results from an enthalpic step in the breakdown of any possible higher order structure, no matter how broad the transition may actually be. There was no deviation from the established baseline up to the temperature where the thermal denaturation of the nucleosome structure sets in. Neither UV-melting nor CD-melting recorded at the two characteristic wavelengths showed any trace of a cooperative conformational change in the temperature region below the main transition.

HIGHER ORDER STRUCTURES IN CHICKEN ERYTHROCYTE CHROMATIN ARE STABILIZED BY ENTHALPY

Chromatin higher order structures in chicken erythrocytes are stabilized by an enthalpic contribution rather than by entropy alone. Quantitative evidence was derived from a systematic spectroscopic and calorimetric study [75] using various nuclear components, e.g. mono-nucleosomes, tetramers/pentamers or soluble chromatin, to determine the chromatin structure of terminally differentiated cells (chicken erythrocytes). These components cover all possible levels of structural complexity and range from isolated nucleosomal core particles to whole cells. Up to the level of soluble chromatin, the only prominent features of the differential scanning calorimetry profile are the independent denaturation of the two main structural domains of the polynucleosomal chain, the linker DNA and the DNA wrapped around the core histones. The contribution of the nucleosomal structure to the denaturation profile of whole nuclei predominated even within staphylococcal nuclease treated nuclei [76–78]. The profile of untreated nuclei (Fig. 8), however, revealed a new feature on the high temperature side (shaded area) which originated from the unperturbed higher order structure of native chromatin. The same enthalpic contribution was also visible in thermal denaturation profiles of whole Friend cells and metaphase chromosomes isolated from these cells but not in hyperacetylated chromosomes. The subfraction of the enthalpic contribution, which we assigned to higher order structural elements, may arise from compaction and topological constraints in the looped domains of chromosomes. They amount to approximately one third of the enthalpy changes

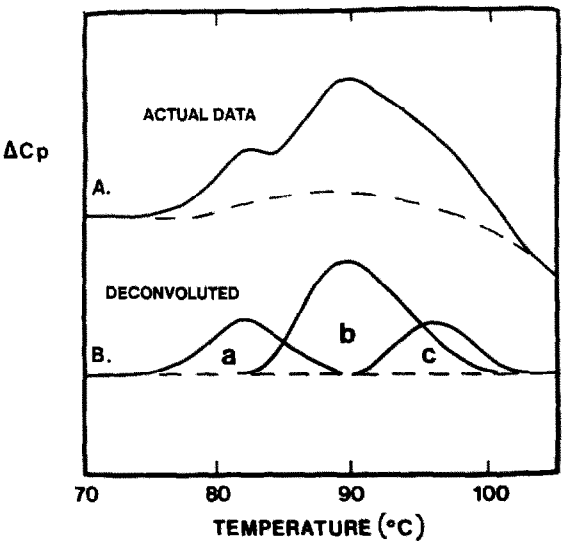

Fig. 8. Heat capacity vs. temperature for soluble chromatin. A, experimental curve; B, deconvoluted set transitions. a, linker DNA; b, core DNA; c, "higher order structure" contribution.

associated with the overall denaturation enthalpy of the polynucleosomal string of beads.

REFERENCES

1 H.-J. Hinz, in I. Jones (Ed.), Biochemical Thermodynamics, 1st edn., Elsevier, Amsterdam, 1979, pp. 116–167 and references cited therein.
2 H.H. Klump, in I. Jones (Ed.), Biochemical Thermodynamics, 2nd edn., Elsevier, Amsterdam, 1988, pp. 100–146 and references cited therein.
3 H.H. Klump, in W. Saenger (Ed.), Landolt Börnstein, Neue Serie, Group VII, Vol. 1C, Biophysik, Springer, Heidelberg, 1990.
4 J.H. Van de Sande, N. Ramsing, M. Germann, W. Elhorst, W. and T. Jovin, Science, 240 (1988) 551–557.
5 P. Privalov, O. Ptitsyn and M. Birshtein, Biopolymers, 8 (1967) 559–571.
6 H.H. Klump, and K. Herzog, Ber. Bunsenges. Phys. Chem., 88(19) (1984) 20–24.
7 J. Collins, and B. Hohn, Proc. Natl. Acad. Sci. U.S.A., 75 (1979) 4242–4247.
8 N. Kleckner, Annu. Rev. Genet., 15 (1981) 341–349.
9 A. Rich, A. Nordheim and A. Wang, Annu. Rev. Biochem., 52 (1984) 791–846 and references cited therein.
10 M.W. Germann, B.W. Kalisch and J.H. Van de Sande, Biochemistry, 27 (1988) 8302–8306.
11 R. Häner and P.B. Dervan, Biochemistry, 29 (1990) 9761–9765.
12 A. Worcel, S. Han and M.L. Wong, Cell, 15 (1978) 969–977.
13 N. Benyajati and A. Worcel, Cell, 9 (1976) 393–407.
14 M. Marsden and U. Laemmli, Cell, 17 (1979) 849–858.
15 P. Privalov, V. Poltnikov and V. Filimonov, J. Chem. Thermodyn., 7 (1975) 41–47.
16 D. Gruenwedel, Biochim. Biophys. Acta, 340 (1974) 14–26.

17 T. Jovin, I. McIntosh, and G. Arnd-Jovin, J. Biomol. Struct. Dyn., 1 (1983) 2157–2168.
18 I. Tinoco, Jr., O. Uhlenbeck and M. Levine, Nature 230 (1971) 362–367.
19 D. Gruenwedel, Biochim. Biophys. Acta, 395 (1975) 246–257.
20 N. Kallenbach, J. Mol. Biol., 37 (1968) 445–456.
21 H.H. Klump and Th. Ackermann, Biopolymers, 10 (1971) 513–522.
22 M. Eigen, Ber. Bunsenges. Phys. Chem., 68 (1964) 889–895.
23 P. Privalov, K. Kafiani and D. Monadselidze, Biofizika, 10 (1965) 393–398.
24 H.C. Longuet-Higgins and B. Zimm, J. Mol. Biol., 2 (1960) 1–15.
25 Ph. Ross, M. Rawitscher and J. Sturtevant, Biopolymers, 3 (1965) 213–223.
26 M. Chamberlin, and D. Patterson, J. Mol. Biol., 12 (1965) 410–424.
27 H.H. Klump, Can. J. Chem., 66 (1988) 804–811 and references cited therein.
28 T. Record, T. Lohman and P. DeHaseth, J. Mol. Biol., 107 (1976) 145–158.
29 R. Jin. K. Breslauer, R. Jones and B. Gaffney, Science, 250 (1990) 543–550.
30 F. Pohl, and T. Jovin, J. Mol. Biol., 67 (1972) 375–384.
31 A. Wang, R. Gessner, G. Van der Marel, J. van Boom and Rich, A. Proc. Natl. Acad. Sci., 82 (1985) 3611–3618.
32 N. Pattabiraman, Biopolymers 25 (1986) 1603–1606.
33 M. Germann, B. Kalisch, R.T. Pon, and J.H. van de Sande, Biochemistry, 29 (1990) 9426–9432.
34 P. Rajagopal and J. Feigon, Nature, 339 (1990) 637–640.
35 G. Manzini, L. Xodo, D. Gasparotto, F. Quadrifoglio, G. van der Marel and J. van Boom, J. Mol. Biol., 213 (1990) in press.
36 L. Xodo, G. Manzini and F. Quadrifoglio, Nucleic Acid Res., 18 (1990) 3557–3564.
37 V. Layamichev, S. Mirkin and M. Frank-Kamenetski, J. Biomol. Struct. Dyn. 3 (1986) 667–669.
38 R. Wells, D. Collier, J. Hanvey, M. Shimizu and F. Wohlrab, Fed. Am. Soc. Exptl. Biol. J., (1988) 2939–2949.
39 J. Völker, D. Botes, G. Lindsey and H.H. Klump, J. Mol. Biol., (1991) in press.
40 J. Marmur and P. Doty, J. Mol. Biol., 5 (1962) 109–120.
41 R. Ornstein and J. Fresco, Biopolymers, 22 (1983) 1979–2000.
42 J. Wang, Trends Biochem. Sci., 5 (1980) 219–223.
43 A. Seidl, Thesis, Regensburg, (1983) p. 37 ff.
44 J. Wang, Cell, 29 (1982) 724–735.
45 J. Wang, J. Mol. Biol., 55 (1971) 523–535.
46 W. Bauer, F. Crick, and J. White, Sci. Am., 242 (1980) 123–133.
47 G.S. Manning, Biopolymers, 11 (1972) 937–948.
48 K. Breslauer, in H. Hinz (Ed.), Chemical Thermodynamic Data for the Biological sciences, Elsevier, Amsterdam, 1986, pp. 123–157.
49 H.H. Klump and D. Maeder, Pure Appl. Chem., 83 (1991) 1357–1388.
50 E. Murrey and M. Eberle, Nucleic Acid Res., 17 (1989) 477–497.
51 P. Sharp, E. Cowe, D. Higgins, D. Shields, K. Wolfe and F. Wright, Nucleic Acid Res. 16 (1988) 8207–8211.
52 R. Grantham, C. Grautier, M. Gouy, M. Jacobzone and R. Mercier, Nucleic Acid Res., 9 (1981) r43–r74.
53 D. Shields and P. Sharp, Nucleic Acid Res., 15 (1987) 8023–8040.
54 H. Grosjean and W. Fiers, Gene, 18 (1982) 199–209.
55 H. Pfizinger, P. Guillemaut, J.H. Weil and D. Pillay, Nucleic Acid Res., 15 (1987) 1377–1386.
56 A. Wada and A. Suyama, FEBS Lett., 188 (1985) 291–294.
57 A. Wada, H. Tachibana, O. Gotoh and M. Takanashi, Nature, 263 (1976) 439–440.
58 S. Pedersen, Eur. Mol. Biol. Organ. J., 3 (1984) 2895–2898.
59 S. Liebhaber, M. Goossens and Y. Kau, Proc. Natl. Acad. Sci. USA, 77 (1980) 7054–7058.

60 D. Cooper, M. Toggart and A. Bird, Nucleic Acid. Res., 11 (1983) 647–658.
61 R. Lathe, J. Mol. Biol., 183 (1985) 1–12.
62 A. Brownlee, Nucleic Acid Res., 17 (1989) 1327–1335.
63 A. Wada and A. Suyama, Prog. Biophys. Mol. Biol., 47 (1986) 113–157.
64 M. Sorensen, CG Kurland and S. Pedersen, J. Mol. Biol., 207 (1989) 365–377.
65 T. Ikemura, Mol. Biol. Evol., 2 (1985) 13–34.
66 E. Murrey, J. Lotzer and M. Eberle, Nucleic Acid. Res., 17 (1989) 477–498.
67 R.D. Blake and S. Lafoley, Biochim. Biophys. Acta, 518 (1971) 233–240.
68 T. Beridze, Satellite DNA, Springer, Heidelberg, (1982) and references cited therein.
69 E. Selker, Trends Biol. Sci., 15 (1990) 103–107.
70 M. Behe and G. Felsenfeld, Proc. Natl. Acad. Sci. USA 78 (1981) 1619–1623.
71 D. Praseuth, L. Perroualt, T. LeDoan, T. Chassignol, N. Thoung and C. Helene, Proc. Natl. Acad. Sci. USA 85 (1988) 1349–1353.
72 W. Weischet, K. Tatchell, K. Van Holde and H. Klump, Nucleic Acid Res., 5 (1978) 139–160.
73 K. van Holde, Chromatin, Springer, Heidelberg, (1989) and references cited therein.
74 B. Cavazza, G. Brizozolara, G. Lazzarini, E. Patrone, M. Piccardo, P. Barboro, S. Parodi and C. Balbi, Biochemistry, 28 (1989) 3220–3227.
75 H.H. Klump, Biophys. Chem., 5 (1976) 363–367.
76 M. Almagor and R.D. Cole, Biochemistry, 28 (1989) 5688–5693.
77 M. Almagor and R.D. Cole, J. Biol. Chem., 262 (1987) 15071–15075.
78 C. Balbi, P. Barboro, M. Piccardo, S. Parodi, B. Cavazza, G. Brizzolara and E. Padrone, in Modulating Factors in Multistage Chemical Carcinogenesis, in P. Pani, A. Columbano and L. Feo (Eds.), Plenum Press, New York, 1990, pp. 254–288.
79 M. Go, J. Phys. Soc. Jpn., 23 (1987) 597–608.